Structured Liquid Droplets as Chemical Sensors that Function Inside Living Cells

Uttam Manna, 1,†,§ Yashira M. Zavala, 1,† Nicholas L. Abbott, 1,‡,* and David M. Lynn, 1,2,*

¹Dept. of Chemical and Biological Engineering, Univ. of Wisconsin–Madison, 1415 Engineering Dr., Madison, WI 53706; ²Dept. of Chemistry, Univ. of Wisconsin–Madison, 1101 University Ave., Madison, WI 53706, USA; [†]Equally contributing author; Email: (N.L.A.) nla34@cornell.edu; (D.M.L.) dlynn@engr.wisc.edu

ABSTRACT: We report that micrometer-scale droplets of thermotropic liquid crystals (LCs) can be positioned inside living mammalian cells and deployed as chemical sensors to report the presence of toxins in extracellular environments. Our approach exploits droplets of LC enclosed in semi-permeable polymer capsules that enable internalization by cells. The LC droplets are stable in intracellular environments, but undergo optical changes upon exposure of cells to low, sub-lethal concentrations of toxic amphiphiles. Remarkably, LC droplets in intracellular environments respond to extracellular analytes that do not generate an LC response in the absence of cellular internalization. They also do not respond to other chemical stimuli or processes associated with cell growth or manipulation in culture. Our results suggest that droplet activation involves the transport and co-adsorption of amphiphilic toxins and other lipophilic cell components to the surfaces of internalized droplets. This work provides fundamentally new designs of biotic-abiotic systems that can report sensitively and selectively on the presence of select chemical agents outside cells, and provides a foundation for the design of structured liquid droplets that can sense and report on other biochemical or metabolic processes inside cells.

Keywords: Liquid Crystals, Polymers, Microcapsules, Cells, Stimuli-Responsive Materials

Introduction

Many types of soft materials can reorganize and respond dynamically to environmental stimuli, including weak external fields and the adsorption of molecules. These events can lead to changes in structure and materials properties that occur at multiple length scales and can, in many cases, amplify weak intermolecular interactions in ways that are technologically useful—for example, to promote remodeling, rupture, or the dissolution of a matrix for applications such as controlled drug delivery, or to produce readily observable signals that can report on local conditions and, thereby, serve as platforms for environmental sensing.

The properties of thermotropic liquid crystals (LCs) are of particular interest in this context.²⁻⁴ Many recent studies have demonstrated that the optical properties of LCs and the behaviors of these structured liquids at interfaces can be exploited to develop sensitive new approaches to chemical and biomolecular sensing.⁵⁻¹² Past studies reveal that small perturbations in interfacial energy that result from the adsorption of analytes at interfaces created between LCs and aqueous phases, for example, can promote changes in the orientational ordering of LCs in ways that correlate to the concentration and structure of adsorbed species and that can be readily detected using polarized light.^{7,13-22} Many different types of aqueous/LC interfaces have been investigated for this purpose,⁵⁻¹² with colloidal 'LC-in-water' droplet-based emulsion systems ^{12,23-30} proving to be particularly versatile. Micrometer-scale droplets of thermotropic LCs suspended in water can report the presence of toxic amphiphiles, such as bacterial endotoxins, at concentrations as low as ~1 pg/mL,¹² and changes in droplet size, interfacial properties, and other parameters can be used to tune the responses, sensitivities, and physical behaviors of these colloidal LC sensors in useful ways.^{12,25}

We reported previously on so-called 'caged' LC droplets, in which small, micrometerscale droplets of LC are physically contained (or 'caged') inside a larger semi-permeable polymer multilayer membrane.31-33 The LC droplets in these 'caged' LC systems undergo diagnostic changes in shape, optical appearance, and rotational mobility upon exposure to small amphiphilic analytes (e.g., surfactants and lipids), 31-33 but are protected from changes in these properties induced by contact with larger species (e.g., proteins) that are too large to pass through the pores in the surrounding polymer 'cage'. This feature makes possible the deployment, characterization, and application of LC droplets in complex environments, including in biological media, in ways that are not possible using conventional (or 'bare') LC droplets. Indeed, past studies demonstrate that caged LCs can be used to report the presence of synthetic amphiphilic analytes in serum-containing cell culture media, 32 and that these membraneencapsulated droplets can be immobilized onto the phospholipid-rich membranes of mammalian cells^{27,32} without (i) promoting orientational transitions in the LC droplets or (ii) inducing substantial cytotoxicity. Those key findings enabled the deployment of arrays of 'wearable' cellimmobilized LC droplet sensors within populations of cells that could be used to report—in real time, in vitro, and at the level of individual cells—on the exposure of cells to environmental toxins or other agents.³²

In view of the well-established sensitivity of LC droplets to the presence of adsorbed amphiphiles, ^{12,23-25} the behaviors of 'caged' LCs reveal a remarkable combination of physical and chemical robustness—properties that we attribute, at least in part, to the presence of the semi-permeable polymer membranes that surround the LC droplets and the partially-filled nature of the capsules (the combination of which creates a 'bare' aqueous/LC interface that is, to a substantial degree, similar to that found in conventional LC-in-water emulsions, but is also

protected from many elements present in the surrounding milieu that might otherwise adsorb onto it). 32 These observations led us to hypothesize that the stability and selectivity conferred by these polymer cages could also provide opportunities to characterize the behaviors of thermotropic LCs inside living cells and, thereby, design new classes of biotic/abiotic systems containing structured liquid droplets that respond to chemical stimuli in more complex ways. Here, we provide first demonstrations that small droplets of thermotropic LCs 'caged' in polymer membranes can be positioned inside living mammalian cells and deployed as chemical sensors. Our results reveal the orientational ordering and optical properties of caged LC droplets to be stable in intracellular environments, and that internalized droplets can rapidly, selectively, and reversibly respond to report the presence of toxins in the extracellular environment (including, remarkably, analytes that do not otherwise generate an LC response in the absence of cellular internalization). This work provides fundamentally new approaches to interface responsive thermotropic LC systems with living mammalian cells. Our results reveal that internalized LC droplets can report sensitively and selectively on the presence of select chemical agents *outside* cells. They also provide a foundation for the design of structured liquid droplets that have the potential to sense and report, with spatial and temporal control, on other biochemical, metabolic, or mechanical processes *inside* cells (e.g., processes associated with the production of fatty acids or other lipophilic agents, etc.) in ways that would be difficult or impossible to achieve using conventional methods and tools.

Materials and Methods

Materials. Branched poly(ethyleneimine) (PEI, M_W ~25,000), 2,2'-azoisobutyronitrile (AIBN), 1-aminodecane (n-decylamine), hexadecyltrimethylammonium bromide (HTAB), sodium dodecylsulfate (SDS), tetrahydrofuran (THF), acetone, and dimethyl sulfoxide (DMSO) were purchased from Sigma Aldrich (Milwaukee, WI). TritonX-100 was purchased from Promega (Fitchburg, WI). SiO₂-Research microparticles (diameter of $5.06 \pm 0.44 \mu m$) were purchased from Bangs Laboratories, Inc. (Indiana, USA). 2-Vinyl-4,4-dimethylazlactone (VDMA) was a gift from Dr. Steven M. Heilmann (3M Corporation, Minneapolis, MN). Tetramethylrhodamine (TMR) cadaverine was purchased from Invitrogen (Oregon, USA). The thermotropic liquid crystal E7 was obtained from Licristal, Japan. Ethanol was purchased from Decon Labs. 3-Dimethylaminopropylamine (99%) was purchased from Acros Organics (New Jersey, USA). 1,2-Distearoyl-sn-glycero-3-phosphocholine (DSPC) was purchased from Avanti Polar Lipids (Alabaster, AL). Dulbecco's modified Eagle's medium (DMEM), minimum essential medium (MEM), Opti-MEM cell culture medium, phosphate-buffered saline (PBS), fetal bovine serum (FBS), trypsin EDTA 0.25% phenol red, Calcein AM, and live/dead cell viability assay kits were purchased from Invitrogen (Carlsbad, CA). Bleach (Clorox) was obtained from Amazon.com, Inc. Poly(2-vinyl-4,4-dimethylazlactone) (PVDMA, $M_W \sim 10,300$; PDI = 3.2) was synthesized by the free-radical polymerization of VDMA, as described previously.³⁴ PVDMA labeled with TMR (1 mol%; referred to from here on as PVDMA_{TMR}) was synthesized as described previously.³⁴ Fluorescently labeled PEI/PVDMA microcapsules and 'caged' LCs were fabricated as previously reported. 31-33 Aqueous dispersions of SiO₂ microparticles were rinsed with acetone and then suspended in acetone prior to use as templates for layer-by-layer deposition. All other

materials were used as received without further purification unless otherwise noted.

General Considerations. Laser-scanning confocal microscopy (LSCM) images were acquired using a Nikon A1-R high-speed confocal microscope and processed using Nikon Instruments Software. Fluorescence microscopy images used for the analysis of live/dead cell assays were acquired using an Olympus IX70 microscope and analyzed using the MetaMorph Advanced version 7.7.8.0 software package (Universal Imaging Corporation). Other fluorescence microscopy images were acquired using an Olympus IX71 inverted microscope (Center Valley, PA). Bright-field and polarized light micrographs of LC emulsions were acquired using a Hamamatsu 1394 ORCAER CCD camera (Bridgewater, NJ) connected to a computer and controlled through SimplePCI imaging software (Compix, Inc., Cranberry Twp., NJ).

Influence of Added Amphiphiles on the Orientational Ordering of Freely-Suspended 'Caged' LCs. The influence of SDS, HTAB, TritonX-100, and DSPC on the orientational ordering and optical appearances of bare LC droplets and 'caged' LC droplets was characterized by adding specified volumes of concentrated solutions of each amphiphile to dispersions of bare and 'caged' LC droplets in deionized water and cell culture media. The optical appearances of the droplets were then characterized using bright-field and polarized light microscopy.

Characterization of 'Caged' LC Droplets Immobilized On and Internalized By Cells. HeLa cells were seeded in confocal dishes ($\phi = 35$ mm) at an initial density of 150,000 cells/mL in 2 mL of growth medium (MEM supplemented with 10% (v/v) fetal bovine serum, 100 units/mL penicillin, and 100 µg/mL streptomycin). Cells were allowed to grow overnight at 37 °C to

approximately 80% confluence before use in subsequent experiments. For experiments involving the use of COS-7 cells, DMEM supplemented with 10% (v/v) fetal bovine serum, 100 units/mL penicillin, and 100 µg/mL streptomycin was used as the growth medium. For experiments involving the use of 3T3 cells, DMEM supplemented with 10% (v/v) newborn calf bovine serum, 100 units/mL penicillin, and 100 µg/mL streptomycin was used as the growth medium. In some experiments, cells were stained using Calcein AM prior to use using the following general protocol: growth medium was aspirated, cells were stained with 2 mL of Calcein AM staining solution (1 µg/mL in PBS) for 45 minutes at 37 °C, and the staining solution was aspirated and replaced with 2 mL of fresh DMEM. For experiments designed to characterize the interactions of 'caged' LCs with cells, a specified volume of a concentrated dispersion of 'caged' LCs was added to cells to achieve a final desired concentration of capsules (typically ~100,000 capsules/mL) and cells were incubated for up to 18 hours. Cells were then rinsed twice using Dulbecco's phosphate buffer solution (DPBS) and fresh medium was added. Cells and 'caged' LC droplets were then characterized using phase contrast, fluorescence, polarized light, and/or confocal microscopy. Live/dead cytotoxicity assays were performed using HeLa cells seeded in 24-well plates at initial densities of 100,000 cells/mL in 500 µL of growth medium. After plating, cells were allowed to grow overnight at 37 °C until they reached ~80% confluence. Culture medium was aspirated, replaced with 500 µL of fresh culture medium prepared with desired concentrations of TritonX-100 or LC-filled capsules, and the cells were incubated at 37 °C for desired lengths of time. After the incubation period, media was aspirated from the wells, cells were rinsed with DPBS, and new media was added. Cytotoxicity assays were then conducted, in replicates of three, using a commercially available fluorescence live/dead assay kit according to the manufacturer's protocol.

Influence of Environmental Challenges on Internalized LC Droplets. Cells containing internalized 'caged' LCs were subjected to a variety of chemical and environmental challenges. All of these experiments were performed using HeLa cells and fluorescently-labeled 'caged' LCs. General descriptions of protocols specific to each type of experiment or environmental condition evaluated are described below.

Influence of added amphiphiles or other media components. For experiments designed to characterize the influence of the addition of synthetic amphiphiles or glucose to the extracellular environment, SDS, HTAB, TritonX-100, or glucose were added to culture wells via pipette to reach desired in-well concentrations. Cells and 'caged' LC droplets were characterized after defined incubation periods using phase contrast, fluorescence, polarized light, and/or confocal microscopy.

Influence of incubation time. For experiments designed to characterize the influence of time on orientational transitions in internalized LC droplets, cells containing internalized 'caged' LCs were maintained in a 37 °C incubator and removed briefly every 24 hours to permit characterization by phase contrast, fluorescence, polarized light, and/or confocal microscopy. Cell culture media was removed and replaced with fresh media every two days.

Influence of environmental temperature. For experiments designed to characterize the influence of environmental temperature on orientational transitions in internalized LC droplets, cells containing internalized 'caged' LCs, prepared as described above, were transferred to incubators pre-adjusted to either 20 °C or 40 °C and incubated for 18 h. Cells and 'caged' LC droplets were then characterized using phase contrast, fluorescence, and polarized light microscopy.

Influence of environmental pH. Experiments designed to characterize the influence of environmental pH on the orientational transitions of internalized LC droplets were conducted by adjusting the pH of the cell culture media to pH 6 or pH 9 using a specified volume of an HCl or NaOH solution. Cells were then incubated for 18 hours at 37 °C, after which cells and 'caged' LC droplets were characterized using phase contrast, fluorescence, and polarized light microscopy.

Influence of glutaraldehyde fixation. Experiments designed to characterize the impact of the chemical fixation of cells on orientational transitions in internalized LC droplets were conducted by incubating cells containing internalized 'caged' LCs in a 2.5% (v/v) glutaraldehyde solution for 30 minutes at 37 °C, followed by rinsing with fresh cell culture media. Cells and 'caged' LC droplets were then characterized using phase contrast, fluorescence, polarized light, and/or confocal microscopy.

Influence of trypsinization and cell detachment. Experiments designed to characterize the influence of trypsinization and the detachment of cells from their underlying substrates on orientational transitions in internalized LC droplets were conducted by adding 1 mL of a solution of trypsin EDTA (0.25%) to cells containing internalized LC-filled capsules and then incubating them at 37 °C for 2 minutes. Cells and 'caged' LC droplets were then characterized using phase contrast, fluorescence, and polarized light microscopy.

Influence of bleaching. Experiments designed to characterize the influence of bleach treatment and cell death on orientational transitions in internalized LC droplets were conducted by adding 100 μL of a concentrated bleach solution (8.25%) to cells containing internalized LC-filled capsules. Cells and 'caged' LC droplets were then characterized using phase contrast, fluorescence, and polarized light microscopy.

Results and Discussion

Caged LCs are Readily Internalized by Mammalian Cells

To characterize the behaviors of LC droplets hosted in intracellular environments, we used 'caged' LC droplets with structures and compositions similar to those we reported on previously for the immobilization of LC droplets onto the surfaces of mammalian cells.³² Briefly, we used reactive/covalent layer-by-layer assembly to fabricate cross-linked PEI/PVDMA multilayers on the surfaces of silica microspheres (~5 µm in diameter), followed by treatment with dimethylaminopropylamine (DMAPA) to react with residual azlactone functionality and install additional protonatable tertiary amine groups on the surfaces of the multilayer coatings. Subsequent removal of the microparticle core resulted in hollow microcapsules (Figure 1A), which were then filled with LC and extracted into water to yield partially-filled capsules (as depicted schematically in Figure 1A-B). For all experiments below, we used capsules partially filled with the nematic LC E7 (Figure 1I), because this LC has a nematic-to-isotropic transition temperature of ~60 °C, which is well above the temperature of 37 °C typically used in mammalian cell culture experiments.

The orientational ordering of the LC droplets in capsules suspended in cell culture media containing 7% serum was first characterized using bright field and polarized light microscopy. As shown in Fig. 1E,G, the LC droplets existed in the so-called 'bipolar' configuration, in which the director of the LC connects two point defects at opposite ends of the droplet (as shown schematically in Figure 1C; point defects are visible as dark spots in the bright field image in Figure 1E). Addition of the cationic surfactant HTAB (to a 50 μ M final concentration) resulted in a rapid transition in the orientational ordering of these caged LC droplets from the initial bipolar configuration to the so-called 'radial' configuration (Figure 1D,F,H), which exhibits a

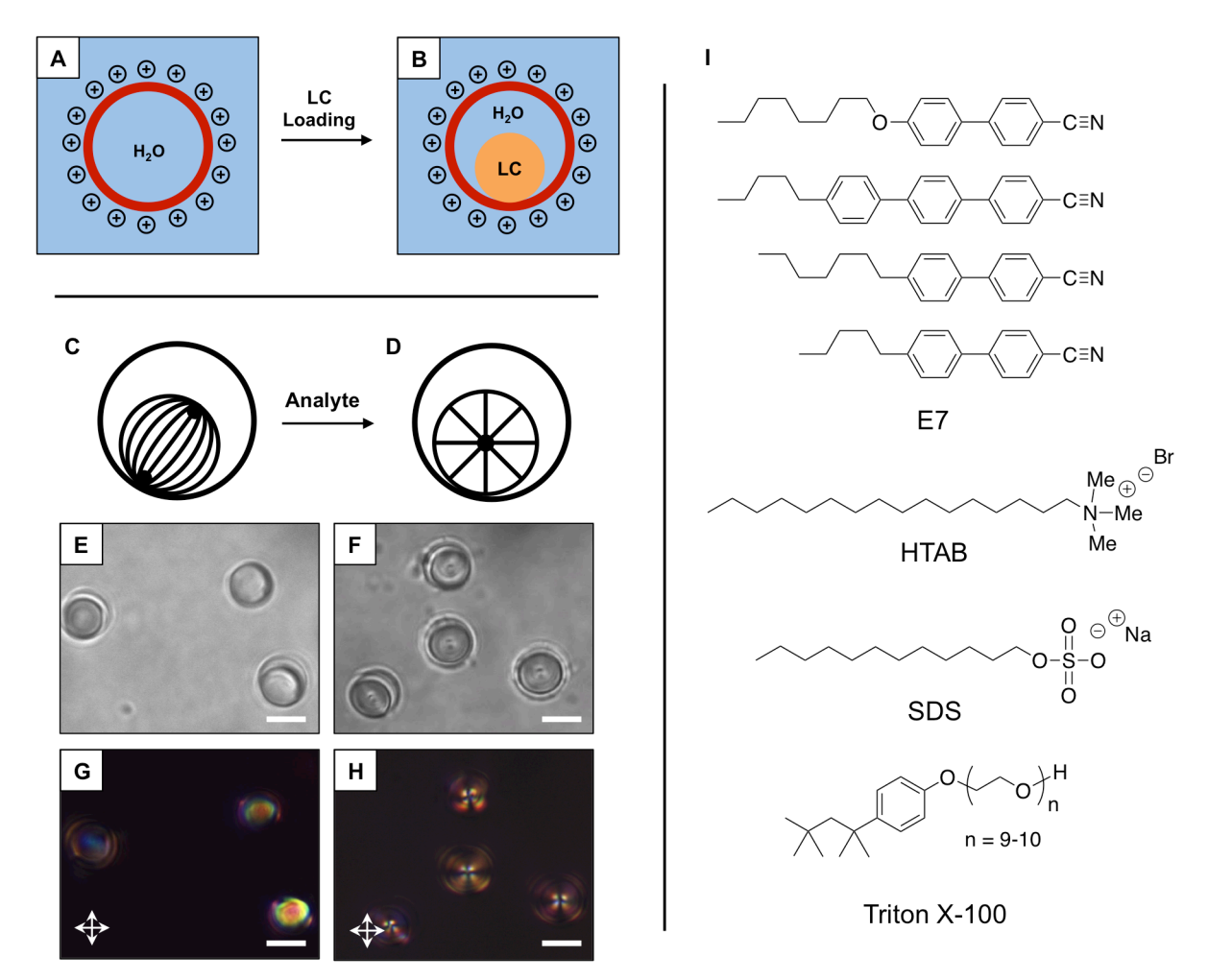


Figure 1: (A-B) Schematic illustrations depicting the fabrication and structure of 'caged' LCs, consisting of covalently-crosslinked and amine-functionalized polymer microcapsules (A; red; depicted in protonated state, see text) partially filled with micrometer-scale droplets of a thermotropic LC (B; yellow). The capsule and 'caged' LC are both shown suspended in water (blue). (C-D) Schematic illustrations showing the director profiles for a 'caged' LC droplet in the bipolar configuration (C) and the transition to a radial configuration (D) promoted by the addition of an analyte. (E-H) Bright-field (E-F) and polarized light (G-H) microscopy images of caged LC droplets suspended in cell culture media before (E,G) and after (F,H) addition of HTAB (50 μm) Scale bars are 5 μm; crossed double-headed arrows indicate the direction of crossed polarizers. (I) Chemical structures of the LC E7 and the amphiphiles HTAB, SDS, and Triton X-100 used in this study.

single defect at the core of the droplet (as shown schematically in Figure 1D; point defects are visible as dark spots near the centers of the droplets in the bright field image in Figure 1F).

We performed a series of experiments to determine whether these caged LCs could be internalized by mammalian cells and, subsequently, whether the LC droplets in these materials could respond to conditions (or changes in conditions) experienced in intracellular environments.

For these studies, we selected two model cell lines (HeLa cells and 3T3 cells) that are known to be able to internalize micrometer-scale objects³⁵ (COS-7 cells used in our prior work do not efficiently internalize micrometer-scale objects on the order of the sizes of the caged LCs used here) and capsules fabricated using fluorescently-labeled PVMDA (PVDMA_{TMR}; see Methods). In a first series of experiments, both bare LC droplets and caged LC droplets were added to cell culture media surrounding HeLa cells growing on tissue culture polystyrene. Cells were allowed to incubate in the presence of bare and caged LC droplets for 18 hours and were then washed once prior to imaging (see Figure S1 of the Supporting Information; see Methods for additional details). In experiments performed using bare droplets, the droplets were readily removed from the system by this washing procedure (as revealed by their absence in Figures S1A-C), indicating that they were not immobilized strongly onto or internalized by the cells. In contrast, caged LC droplets remained associated with the cells after washing (as revealed by their presence in the bright field, fluorescence, and cross polarized microscopy images shown in Figures S1D-F). These results indicate that the polymeric multilayers surrounding the caged LC droplets play an important role in mediating association with cells, likely through initial electrostatic interactions between the positively charged multilayers and the cell surface, as described in past studies.³²

We performed an additional series of experiments to (i) determine whether the cell-associated caged LC droplets described above were located on the surfaces or inside the cells, and (ii) estimate the percentage of cells that internalized the caged LC droplets under these conditions. In initial studies, we used a standard Trypan blue assay to characterize the locations and extents of internalization of caged LC droplets. Trypan blue acts as a fluorescence quencher, and thus quenches the fluorescence signal of other fluorescent molecules with which it comes in contact. Trypan blue cannot penetrate intact cell membranes, however, and, thus, the

presence of Trypan blue added to cell culture media does not influence the fluorescence emission of fluorescent molecules located inside cells. 36,37 We added Trypan blue to media surrounding HeLa cells incubated with caged LC droplets labeled with tetramethylrhodamine (TMR; red) for 18 hours, as described above, and characterized the quenching of fluorescence signal associated with the caged LCs using a fluorescence microscope, as shown in Figure 2C-D, to differentiate between immobilized (Figure 2A) and internalized (Figure 2B) capsules. In the images in Figure 2C-D, arrowheads mark the locations of internalized caged LCs (revealed by the presence of observable fluorescence in Figure 2D), and asterisks mark the locations of caged LCs that were immobilized or cell-associated, but not internalized (as revealed by the absence of observable fluorescence in Figure 2D). The results of similar experiments performed using 3T3 cells and COS-7 cells are shown in Figure S2. For 3T3 cells, as shown in Figure S2B,D we also observed capsules that were not quenched, indicative of internalization by this cell line. In contrast, for COS-7 cells, a cell line that, as noted above, does not efficiently internalize microscale objects, all capsules were quenched by Trypan blue (as shown in Figure S2A,C), suggesting that caged LCs are not readily internalized by this cell line.

We also used confocal microscopy to confirm and further characterize the internalization of TMR-labeled caged LC droplets after 18 hours of incubation with HeLa cells (as shown in Figure 2E). For these experiments, HeLa cells were labeled with Calcein AM (a live cell stain; green signal) and Hoechst (a nuclear stain; blue signal) prior to imaging. The results shown in Figure 2E (which shows fluorescence confocal images of *xy*-, *yz*- and *xz*- projections overlaid on a corresponding bright-field image; LC droplets contained within the microcapsules are visible as white/gray) show two spherical and intact caged LCs located inside a single cell.

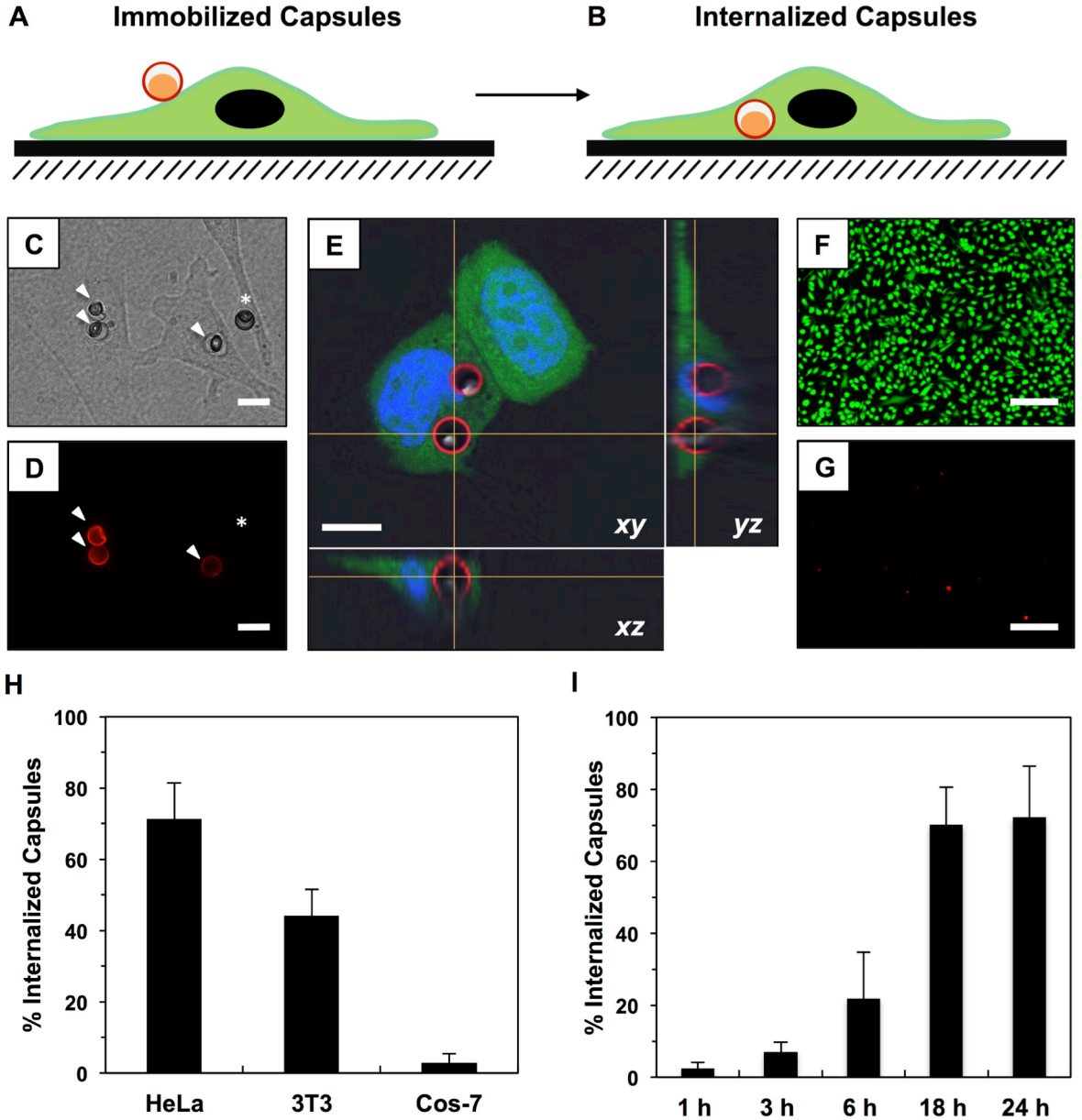


Figure 2: Schematic illustrations showing a 'caged' LC droplet (A) immobilized on the membrane of a mammalian cell and (B) after internalization by a cell. (C-D) Bright-field (C) and fluorescence (D) microscopy images showing 'caged' LC droplets after incubation in culture wells containing HeLa cells for 18 hours, followed by treatment with trypan blue. 'Caged' LCs were fabricated using microcapsules labeled with tetramethylrhodamine (TMR; red). White arrowheads mark the locations of internalized 'caged' LCs; asterisks mark the locations of 'caged' LCs that were not internalized (scale bar = 10 µm). (E) Laser scanning confocal microscopy images of two HeLa cells, one of which contains two internalized 'caged' LCs. Cells were treated with Calcein AM (green) and Hoechst (blue), to stain the cytosol and nuclei, respectively, prior to imaging. 'Caged' LCs were fabricated using microcapsules labeled with tetramethylrhodamine (TMR; red). The fluorescence confocal image is overlayed on a corresponding bright-field image; LC droplets contained within the microcapsules are visible in white/gray. Scale bar = 10 µm. (F-G) Low-magnification fluorescence microscopy images (4X; scale bar = 0.5 mm) of HeLa cells incubated in the presence of 'caged' LC droplets for 18 hours. Cells were stained with Calcein AM (F; green) and ethidium homodimer (G; red) to identify live and dead cells, respectively, prior to imaging. (H) Plot showing the percentages of HeLa, 3T3, and COS-7 cells that internalized at least one 'caged' LC over a period of 18 hours. (I) Plot showing the percentage of HeLa cells that internalized at least one 'caged' LC as a function of time for periods ranging from one to 24 hours.

Additional confocal microscopy results shown in Figure S4D reveal that individual cells can internalize as many as five caged LCs. Figure S4 also shows images of internalized capsules that appeared to be crumpled or broken (Figure S4B-C), as well as an image of a capsule that was immobilized on the outer surface of a cell, but not internalized (Figure S4A; for this experiment, capsules were incubated with cells for one hour instead of 18 hours). Figure S5 shows confocal microscopy images of 3T3 cells (Figure S5A) and COS-7 cells (Figure S5B) incubated with caged LC droplets for 18 hours, showing internalized and immobilized capsules, respectively. These results are consistent with other observations arising from experiments using Trypan blue, as discussed above, indicating that 3T3 cells can internalize caged LCs, but COS-7 cells generally do not.

Additional studies using Trypan blue permitted us to characterize the time dependence of capsule internalization in HeLa cells and characterize differences in the extents to which caged LCs were internalized in larger populations of HeLa, 3T3, and COS-7 cells. For these experiments, caged LCs were incubated with cells (at a concentration of 10⁵ capsules/mL) for times ranging from 1 h to 24 h, and the number of cells that internalized at least one capsule was characterized, as determined by the identification of un-quenched capsules, by fluorescence microscopy. As shown in Figure 2I, the number of cells internalizing at least one capsule increased gradually as a function of time, and reached a maximum of ~70% after 18 h of incubation; the percentage of cells internalizing at least one capsule did not increase significantly at longer incubation times. Whereas ~70% of HeLa cells internalized caged LC droplets after incubation for 18 hours, only ~45% of 3T3 cells internalized caged LC droplets under otherwise identical conditions, as shown in Figure 2H. The number of COS-7 cells internalizing at least one caged LC droplet was negligible. Finally, we note that the results of fluorescence-based

live/dead assays revealed that caged LC droplets were not substantially cytotoxic under these conditions (Figure 2F-G) or when incubated for prolonged periods (e.g., for up to 72 h; Figure S3).

Internalized LC Droplets Respond Selectively to Amphiphilic Toxins in Cellular Environments

We next characterized the orientational ordering of the LC droplets in caged LCs internalized by HeLa cells using polarized light microscopy. Figure 3A-B shows representative bright field (Figure 3A) and polarized light (Figure 3B) microscopy images of an internalized caged LC, and suggest the caged LC droplet to be present in the bipolar state (the typical boojum defects that are present in bipolar LC droplets, as discussed above, could not be observed clearly in internalized caged LC droplets (Figure 3A), but the pattern of optical birefringence shown in Figure 3B is indicative of a droplet in the bipolar configuration; additional images included in Figure S6 also show examples of internalized droplets in this configuration; in the discussion below, we use the term 'bipolar' to describe the configurations of droplets exhibiting these optical appearances). This result suggests that the orientation of the LC in these droplets, which is initially present in the bipolar state (prior to addition to cells, and in the extracellular environment), is preserved, or at least does not transform to a radial configuration, upon transport to the intracellular environment. We regard this result as notable in view of (i) the documented sensitivity of the configurations of LC droplets to the presence of amphiphilic species^{12,25,38} and (ii) the likelihood that these caged LCs come into close contact with lipid membranes and other cell components during internalization.

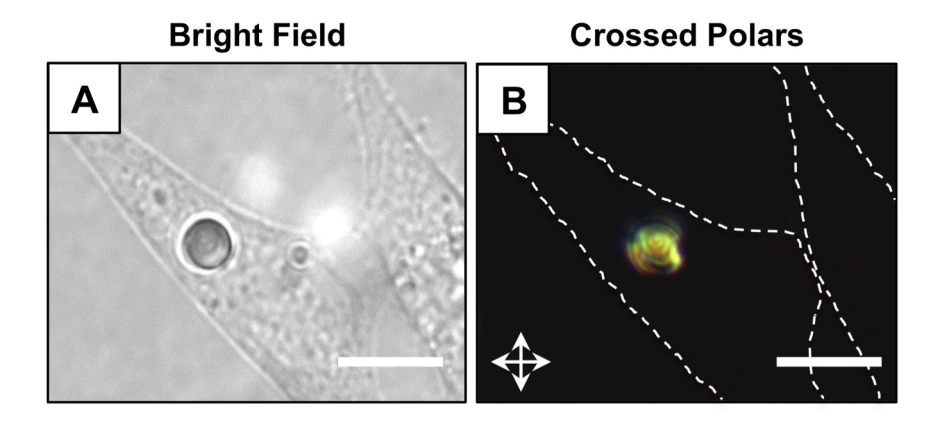


Table 1: Effect of Stimulus on Configuration of LC

Stimulus/Condition	Config. Before	Config. After
Incubation Time (7 days)	Bipolar	Bipolar
pH (6 to 10)	Bipolar	Bipolar
Temperature (20 to 40°C)	Bipolar	Bipolar
Media Composition (Glucose)	Bipolar	Bipolar
SDS (50 µM; Anionic)	Bipolar	Radial
HTAB (50 μM; Cationic)	Bipolar	Radial
Triton X (0.1 mM; Non-Ionic)	Bipolar	Radial
Glutaraldehyde (Fixation)	Bipolar	Bipolar
Trypsinization/Detachment	Bipolar	Bipolar
Bleach (Dead Cells)	Bipolar	Bipolar

Figure 3: Bright-field (A) and polarized light (B) microscopy images showing a 'caged' LC internalized by a HeLa cell (the directions of the polarizers are indicated by the crossed double-headed arrows). The image shown in (B) reveals that the bipolar configuration of the encapsulated LC droplet is retained after internalization. Table 1 shows the configurations of internalized 'caged' LCs both before and after exposure to various chemical or environmental conditions. Dotted white lines indicate the approximate locations of cell borders determined from corresponding bright-field images. Scale bars = $10 \mu m$.

Table 1, shown in Figure 3, summarizes the results of a series of different experiments designed to characterize the impact of various environmental conditions and induced physical, mechanical, or chemical cell stresses on the orientational ordering of caged LC droplets internalized by HeLa cells. These results reveal the LC droplets to remain in the bipolar

configuration after internalization inside cells for up to seven days. Based on these observations, we can conclude that the orientational ordering of caged LC droplets remains unchanged by physical and mechanical forces experienced during cell division and proliferation. We also characterized the effects of physical and chemical changes including chemical fixation by glutaraldehyde and the exposure of cells to changes in pH (over the range of 6 to 10), changes in temperature (from 20° to 40°), and changes in media composition (e.g., the addition of glucose) that deviate from standard cell culture conditions. In all cases, the LC droplets in the caged LCs remained in the bipolar state (Table 1). These internalized LC droplets were also found to remain in the bipolar state after trypsinization and detachment from the surface, a transformation that promotes substantial physical deformation and changes in cell shape as cells that are spread flat on a surface bleb and detach to adopt spherical shapes, and upon re-seeding and attachment to other secondary surfaces (Table 1). Treatment of cells with bleach, which results in cell death, the disruption of the plasma membrane, and the subsequent exposure of the droplets to many other cell parts and components that they are not in contact with in a healthy intact cell, also did not result in deviations from bipolar configurations (Table 1).

In contrast to the results discussed above, we observed the bipolar configurations of LC droplets internalized in HeLa cells to transform rapidly to radial configurations upon the addition of SDS (a model anionic surfactant; at 50 μ M), HTAB (a model cationic surfactant; at 50 μ M), or TritonX-100 (a model non-ionic surfactant; at 0.1 mM) to the extracellular culture medium (see entries in Table 1, and additional images in Figure S6; the chemical structures for these amphiphiles are shows in Figure 11). Past reports have demonstrated that ionic surfactants such as SDS and HTAB can trigger changes in the orientational ordering of LC droplets from bipolar to radial. ^{32,33} In view of those past results, the results of this current study suggest that these

surfactants are able to be transported rapidly across the cellular membrane and that they can adsorb to the LC-aqueous interfaces of internalized caged LC droplets in ways that can lead to bipolar-to-radial transitions. Interestingly, we found HTAB to trigger bipolar-to-radial transitions in LC droplets internalized by cells at lower concentrations (e.g., at 50 μ M) than those required to promote equivalent transitions in caged LC droplets immobilized on the membranes of cells (Figure S8; we return to this observation again below).

We note further, in this context, that TritonX-100 does not trigger bipolar-to-radial transitions, at concentrations of up to 1.0 mM, in bare LC droplets or caged LCs in either water or cell culture media (see Figures S8 and S9, Table 2 of Figure 4, and results of past studies³¹) or in caged LCs immobilized on cell membranes (Figure 4A-B). It is thus notable, and was unexpected, in this context, that the addition of TritonX-100 (at a concentration of 0.1 mM that is below the critical micelle concentration (cmc = 0.24mM)³⁹ for this surfactant) can lead to a rapid bipolar-to-radial transition in internalized LC droplets (Figure S5G-I and Figure 4C-D). The polarized light microscopy images in Figure 4A-B show that the configuration of the LC droplets in immobilized caged LCs remained in the bipolar configuration after the addition of TritonX-100 to the cell culture medium. In contrast, the polarized light microscopy images in Figure 4C-D show that the configuration of the LC droplets in internalized caged LCs transformed to a radial configuration after the addition of TritonX-100 to the cell culture medium. These results establish that bipolar-to-radial transitions are only promoted by the addition of TritonX-100 to the extracellular environment if the LC droplets have been internalized by cells. Our results reveal these TritonX-100-triggered bipolar-to-radial transformations of internalized LC droplets to occur rapidly (e.g., almost all transformations are observed to be complete within approximately one minute after the addition of TritonX-100 to the extracellular culture medium).

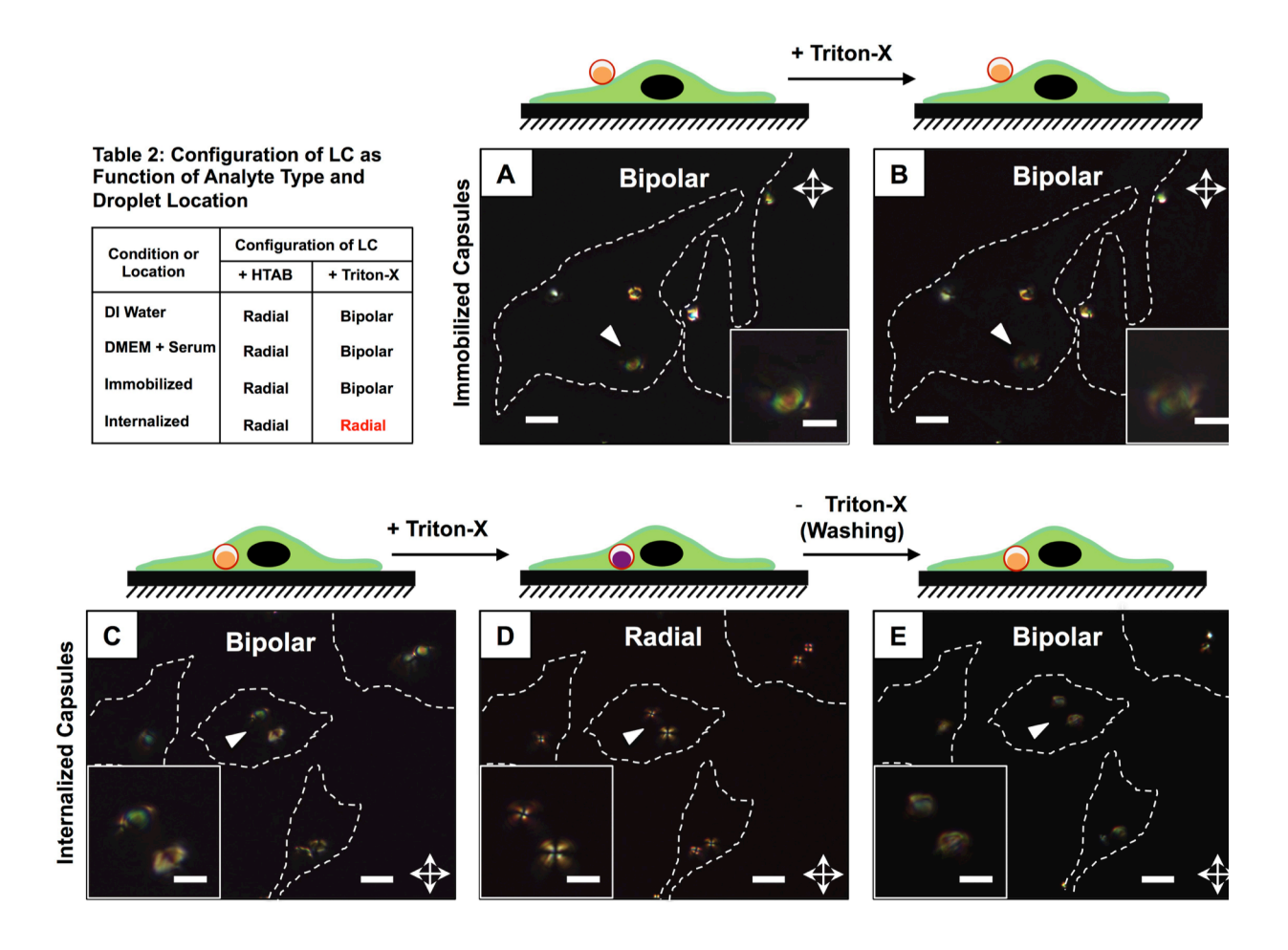


Figure 4: (A-E) Polarized light microscopy images showing immobilized (A-B) or internalized (C-E) 'caged' LCs; the directions of the polarizers are indicated by the crossed double-headed arrows. Immobilized droplets remained in the bipolar configuration before (A) and after (B) the addition of TritonX-100 (0.1 mM) to the cell culture medium. In contrast, internalized droplets were initially present in bipolar configurations (C), but transitioned rapidly to radial configurations (D) after the addition of TritonX-100 (0.1 mM) to the cell culture medium. These droplets returned to the bipolar configuration (E) after removal of media containing TritonX-100 and replacing it with fresh culture media (see text). In each panel, the LC droplets shown in the inset are indicated by the location of the white arrowhead; dotted white lines indicate the approximate locations of cell borders determined from corresponding bright-field images. Table 2 shows the configurations of 'caged' LC droplets in different environments upon exposure to HTAB (50 μM) or TritonX-100 (0.1 mM). Scale bars = 10 μm (5 μm for insets).

Past studies have demonstrated that the surfactant-induced ordering of LC droplets can be reversible.³⁸ The results of our present studies (shown in Figure 4D-E) demonstrate that the bipolar-to-radial transformations of internalized LC droplets triggered by TritonX-100 are also reversible upon the removal of TritonX-100 from surrounding culture media (e.g., by simply

rinsing cell culture dishes with fresh media; see resulting radial-to-bipolar transitions in droplets shown in Figure 4D-E). These radial-to-bipolar transformations of internalized LC droplets also occurred rapidly (e.g., almost all transformations are observed to be complete within approximately one minute after the removal of TritonX-100 and replacement with fresh culture medium). After this rinsing process, transitions from bipolar configurations back to radial configurations could be affected again by the re-addition of TritonX-100 to the culture medium; under these conditions, transformations were observed to occur more rapidly (e.g., over a period of approximately 30 seconds after the re-addition of TritonX-100) than the transformations of droplets that had not been previously exposed to TritonX-100. This reversible switching of the orientational ordering of internalized LC droplets could be repeated up to five times (data not shown). Finally, Figure S7 shows fluorescence microscopy results of a live/dead assay in which HeLa cells were incubated with TritonX-100 for 10 minutes at different concentrations raging from 0 to 1 mM. These results demonstrate that TritonX-100 is not substantially cytotoxic to HeLa cells at a concentration of 0.1 mM under the conditions used in these experiments. The cytotoxicity of TritonX-100 was observed to increase at higher concentrations under these conditions.

Additional Characterization of the Response of Internalized LCs to Non-Ionic Amphiphiles

The responses of caged LC droplets to the addition of Triton-X to cell culture media exhibited by immobilized droplets are completely different from those of droplets immobilized on cell membranes. In view of the results of current experiments, the results of past studies described above, and the complexity of this cell-based system, we consider it unlikely that these transformations are mediated by the transmembrane diffusion and adsorption of TritonX-100

alone at the aqueous/LC interfaces of these caged LCs. In the sections below, we consider three general pathways through which these transformations could be triggered.

One possibility is that the addition of TritonX-100 to the extracellular environment stimulates the intracellular production of compounds or metabolites that accumulate at aqueous/LC interfaces at concentrations and in forms that are capable of promoting bipolar-to-radial transformations. Although it is possible that these transformations could be triggered in this manner, we consider this possibility to be less likely, in general, in view of the rapid manner in which changes in ordering occur and the rapid rate at which these transformations can be reversed by the simple removal of TritonX-100 from the extracellular medium. We note that the notion that such 'biochemical' routes could be possible is nevertheless attractive, in the broad view, from the standpoint of intracellular sensing, and raises the possibility that the bipolar droplet platform reported here could potentially be tailored to respond selectively to specific intracellular analytes produced by cells.

A second possibility is that the addition of TritonX-100 perturbs the cell and promotes changes in cell shape or internal morphology that deform the LC droplets and promote subsequent bipolar-to-radial transitions. This possibility follows broadly on past demonstrations in the literature that configurational transitions in LC droplets can be triggered by deforming them under flow. We hypothesized that physical changes in cell morphology (e.g., contraction or expansion of the cell, etc.) could induce transformations that result in changes in LC droplet configuration. To provide insight into the potential for this possibility to occur, we used confocal microscopy to characterize changes in the morphologies of HeLa cells containing internalized capsules upon the addition of TritonX-100. Figure 5A shows the morphology of a cell containing two internalized caged LC droplets prior to addition of TritonX-100, and Figure 5B

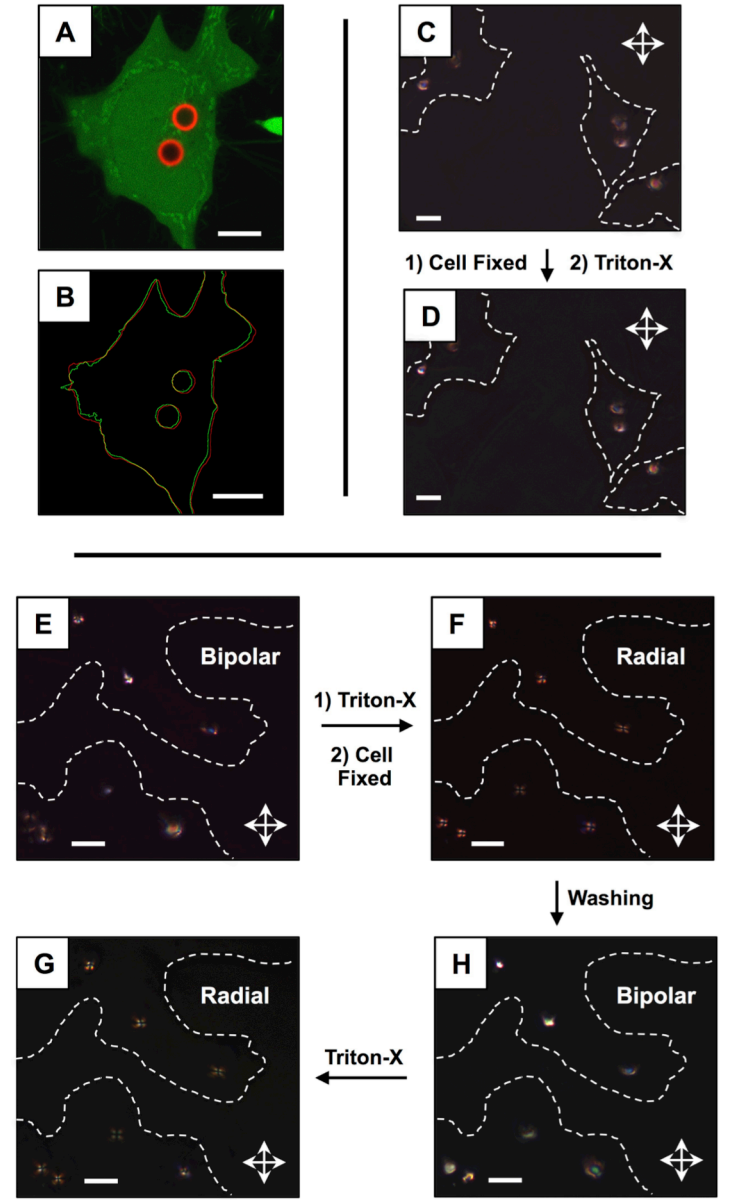


Figure 5: (A) Laser scanning confocal microscopy z-section of a HeLa cell containing two internalized 'caged' LCs before treatment with TritonX-100 (cytosol is stained green; microscapsules are labeled red). (B) Image showing the outline/perimeter of the cell shown in (A) prior to the addition of TritonX-100 (red line) and after the addition of TritonX-100 (green line) as determined by image analysis of confocal microscopy images. (C-H) Polarized light microscopy images of cells containing internalized capsules before and after various chemical or environmental stimuli (the directions of the polarizers are indicated by the crossed double-headed arrows). Panels C and D show cells containing internalized LC droplets prior to treatment (C) and then after a step consisting of first fixing with 2.5% (v/v) glutaraldehyde and then treating them with TritonX-100 (0.1 mM) (D). The image in panel (D) reveals the LC droplets to remain in the bipolar configuration. Panels E-G show LCfilled capsules inside untreated cells (E) and then the same droplets/cells after a step consisting of first subjecting the cells to TritonX-100 (0.1 mM) and then glutaraldehyde fixation (F; the reverse of the sequence shown in the experiment depicted in panels (C-D)). This treatment resulted in the transition of the LC droplets from bipolar to radial configurations. Removal of the X-100 from the cells in (F) by washing promoted a transition of the LC droplets from a radial back to a bipolar state (H). Exposure to additional TritonX-100 resulted in transitions in the LC droplets back to radial configurations (G). Dotted white lines indicate the approximate locations of cell borders determined from corresponding bright-field images. Scale bars = 10 μm (5 μm for insets).

compares the locations of the perimeters of the cell and caged LC droplets before and after the addition of TritonX-100. No gross changes in cell shape were observed. Although it is possible that there are changes in cell shape or the shapes of the internalized droplets that are not revealed by these imaging methods, these results suggest that changes in bipolar-to-radial transformations are not likely to be caused by large changes in cell shape or morphology. This view is supported further by the results of other experiments described above and shown in Table 1, in which the trypsinization and re-seeding of cells did not promote changes in the orientation of internalized LC droplets.

A third possibility is that TritonX-100 facilitates the transport of other cellular components (e.g., lipids, or lipid assemblies and co-assemblies) that are not otherwise mobile or accessible to the aqueous/LC interfaces of internalized LC droplets. In this scenario, for example, the transport of TritonX-100 across cell membranes and through cells could be envisioned to associate with other cellular components (e.g., components of cell membranes or other amphiphilic species that could either be adsorbed on the polymer cages or be accessible in other locations in the cellular environment) that are subsequently transported to the interfaces of the LC droplets in ways that might not otherwise occur. To provide insight into this possibility, we performed a series of additional experiments (Figure 5C-D) in which HeLa cells containing internalized caged LC droplets were first chemically fixed by treatment with a 2.5% (v/v) glutaraldehyde solution. After fixation, TritonX-100 (0.1 mM) was added to the extracellular environment. Surprisingly, and in contrast to what is observed when TritonX-100 is added to live cells containing internalized LC droplets, the bipolar internalized caged LC droplets in these fixed cells remained in the bipolar state after the addition of TritonX-100 (Figure 5C-D; compare to results shown in Figure 4C-D).

We note here that the retention of the LC droplets in the bipolar configuration in these fixed cells after the addition of TritonX-100 is consistent with the possibility of restricted transport of key cellular components during diffusion of TritonX-100 through the fixed cell membrane, but also the restricted transport of TritonX-100 itself through the cell membranes of fixed cells. With respect to the latter issue, we note further that otherwise identical control experiments performed using HTAB (which, as described above, can trigger bipolar-to-radial orientational transitions in bare LC droplets) instead of TritonX-100 (which is unable to trigger these transitions in bare LC droplets) resulted in a rapid bipolar-to-radial transition in internalized LC droplets in fixed cells (Figure S10), suggesting that small-molecule surfactants are able to gain access to the aqueous/LC interfaces of immobilized droplets in fixed cells. We also performed an additional series of experiments, with results shown in Figure 5E-G, in which cells containing internalized caged LC droplets were (i) first treated with 0.1 mM TritonX-100, which resulted in a bipolar-to-radial transition in the LC droplets, and then (ii) cells containing these radial droplets were fixed with 2.5% glutaraldehyde. As expected, the orientational configuration of the LC droplets remained unaffected by fixation, as shown in Figure 5F (that is, the droplets remained in the radial configuration after fixation). However, upon the rinsing of these fixed cells with fresh cell culture media to remove TritonX-100 from the extracellular environment, an orientational transition from radial to bipolar was observed, as shown in Figure 5H. Moreover, these now-bipolar LC droplets were found to be responsive to the further readdition of TritonX-100 to the cell culture media, and changed from bipolar to radial, as shown in Figure 5G, under these conditions.

The outcomes of these experiments are consistent with the following conclusions: (i) the fixing of cells containing bipolar LC droplets renders the LC droplets insensitive to the addition

of TritonX-100 to the surrounding cell culture media, (ii) the transport of added small-molecule surfactants from cell culture media to the internalized LC droplets is not is substantially restricted by fixation, and (iii) the fixing of cells containing radial LC droplets allows further reversible transitions in orientational ordering (from bipolar to radial, and the reverse) upon the addition or subtraction of TritonX-100. Thus, overall, the results of these studies are broadly consistent with the possibility that the addition of TritonX-100 facilitates the transport of lipids or other cellular components (or assemblies or combinations and co-assemblies of TritonX-100 and these components) to aqueous/LC interfaces of the LC droplets in ways that promote changes in orientational ordering. Additional tentative support for this co-adsorption hypothesis is provided by the results of a model experiment in which DSPC (a model lipid that is, by itself, unable to trigger bipolar-to-radial transitions in bare LC droplets) was added to caged LC droplets suspended in water. The configuration of the LC droplets remained bipolar, as shown in Figure S11D-F. However, a transition from bipolar to radial configurations was observed upon the addition of TritonX-100 to caged LCs suspended in the presence of DSPC (Figure S11G-I). This result suggests that TritonX-100, which alone cannot trigger bipolar-to-radial transitions, can solubilize and transport DSPC, which, by itself, also cannot trigger bipolar-to-radial transitions, to the caged LC droplets where they can be absorbed at the aqueous/LC interface to induce orientational transitions from bipolar to radial configurations. Support for this broader hypothesis is also provided by the results discussed above and shown in Figure S8, which show that HTAB can promote bipolar-to-radial transitions in internalized droplets at concentrations that are lower than those required to promote similar transitions in droplets in extracellular environments.

Summary and Conclusions

The work reported here demonstrates that droplet-based LC sensors can be internalized by living mammalian cells, and that internalized LC droplets can report on the presence or absence of toxic amphiphiles in surrounding environments. Micrometer-scale droplets of bare LC droplets are not readily internalized by mammalian cells. In contrast, droplets of LC that are caged in semi-permeable polymeric capsules can be internalized by HeLa cells and 3T3 cells when they are added to cellular environments in vitro. Characterization by polarized light microscopy revealed the orientational ordering and optical properties of these caged LC droplets to be remarkably stable in intracellular environments, but that the droplets undergo transitions from a bipolar to a radial configuration when cells are exposed to synthetic amphiphiles. These optical transitions occur rapidly, selectively, and reversibly, and can be readily observed in real time using polarized light microscopy. Remarkably, LC droplets in intracellular environments were observed to respond to the presence of added extracellular analytes that do not otherwise generate an LC response in the absence of cellular internalization. Internalized droplets also did not respond to other common chemical and environmental stimuli, including changes in pH, temperature, or the addition of chemical fixing agents, or when cells experienced physical and mechanical forces typically associated with cell growth, metabolism, or handling in culture. When combined, our results are consistent with a physical picture that involves the transport and co-adsorption of externally added toxins and other lipophilic cell components to the surfaces of internalized droplets, and not changes in cell shape or metabolism that could occur in response to exposure to toxic agents.

Additional studies will be required to understand the nature of the transitions in these caged LC droplets in intracellular environments more completely, and to define the range of

different analytes and environmental conditions to which they do or do not respond (or to which they may respond selectively or reversibly/irreversibly). Overall, however, the work reported here provides new approaches to interface responsive thermotropic LC systems with living cells and fundamentally new biotic/abiotic systems that can report sensitively and selectively on the presence of toxins outside cells. This work also provides a platform for the design of structured liquid droplets that could, with further development, be positioned inside cells to report on changes in intracellular activity or other chemical, biochemical, or mechanical inputs experienced by cells that would be difficult to observe or measure using existing methods and analytical tools.

Acknowledgment. This work was supported by the NSF through grants to the UW-Madison Materials Research Science and Engineering Center (MRSEC; DMR-1720415) and the Office of Naval Research (N00014-14-1-0791). Facilities used in the research were also supported by the Wisconsin MRSEC. Y. M. Z. acknowledges the Graduate Research Scholars (GERS) program at UW-Madison for a graduate fellowship. We thank Rebecca Carlton and Xiaoguang Wang for technical advice and many helpful discussions.

Supporting Information. Additional characterization of bare and caged LC droplets in the presence of cells, inside cells, and in the presence or absence of various synthetic amphiphiles (PDF). This material is available free of charge via the Internet.

References

- Present address: §U. M.: Department of Chemistry and Centre for Nanotechnology, IIT-Guwahati, Assam 781039, India
- Present address: [‡]N. L. A.: Department of Chemical and Biomolecular Engineering, Cornell Univ., Ithaca, NY 14853, United States
- 1. Hamley, I. W., Introduction to Soft Matter: Synthetic and Biological Self-Assembling Materials, Revised Edition. John Wiley & Sons, Ltd.: West Sussex, England, 2007.
- 2. Drzaic, P. S., Liquid Crystal Dispersions / Ed. Paul S. Drzaic. World scientific: Singapore, 1995.
- 3. Castellano, J. A., Liquid Gold: The Story of Liquid Crystal Displays and the Creation of an Industry. World Scientific Publishing Company: 2005; pp 1-302.
- 4. Yang, D. K.; Wu, S. T., Fundamentals of Liquid Crystal Devices. John Wiley & Sons: New York, 2006.
- Gupta, V. K.; Skaife, J. J.; Dubrovsky, T. B.; Abbott, N. L. Optical Amplification of Ligand-Receptor Binding Using Liquid Crystals. *Science* 1998, 279, 2077-2080.
- Shah, R. R.; Abbott, N. L. Principles for Measurement of Chemical Exposure Based on Recognition-Driven Anchoring Transitions in Liquid Crystals. *Science* 2001, 293, 1296-1299.
- 7. Brake, J. M.; Daschner, M. K.; Luk, Y. Y.; Abbott, N. L. Biomolecular Interactions at Phospholipid-Decorated Surfaces of Liquid Crystals. *Science* **2003**, *302*, 2094-2097.

- 8. Kirchner, N.; Zedler, L.; Mayerhofer, T. G.; Mohr, G. J. Functional Liquid Crystal Films Selectively Recognize Amine Vapours and Simultaneously Change Their Colour. *Chem. Commun.* **2006**, 1512-1514.
- 9. Price, A. D.; Schwartz, D. K. DNA Hybridization-Induced Reorientation of Liquid Crystal Anchoring at the Nematic Liquid Crystal/Aqueous Interface. *J. Am. Chem. Soc.* **2008**, *130*, 8188-8194.
- 10. Bi, X. Y.; Hartono, D.; Yang, K. L. Real-Time Liquid Crystal pH Sensor for Monitoring Enzymatic Activities of Penicillinase. *Adv. Funct. Mater.* **2009**, *19*, 3760-3765.
- Xue, C. Y.; Khan, S. A.; Yang, K. L. Exploring Optical Properties of Liquid Crystals for Developing Label-Free and High-Throughput Microfluidic Immunoassays. *Adv. Mater.* 2009, 21, 198.
- Lin, I. H.; Miller, D. S.; Bertics, P. J.; Murphy, C. J.; de Pablo, J. J.; Abbott, N. L. Endotoxin-Induced Structural Transformations in Liquid Crystalline Droplets. *Science* 2011, 332, 1297-1300.
- 13. Brake, J. M.; Mezera, A. D.; Abbott, N. L. Effect of Surfactant Structure on the Orientation of Liquid Crystals at Aqueous-Liquid Crystal Interfaces. *Langmuir* **2003**, *19*, 6436-6442.
- 14. Hu, Q. Z.; Jang, C. H. Using Liquid Crystals to Report Molecular Interactions between Cationic Antimicrobial Peptides and Lipid Membranes. *Analyst* **2012**, *137*, 567-570.
- 15. Sidiq, S.; Verma, I.; Pal, S. K. pH-Driven Ordering Transitions in Liquid Crystal Induced by Conformational Changes of Cardiolipin. *Langmuir* **2015**, *31*, 4741-4751.
- Alino, V. J.; Sim, P. H.; Choy, W. T.; Fraser, A.; Yang, K. L. Detecting Proteins in Microfluidic Channels Decorated with Liquid Crystal Sensing Dots. *Langmuir* 2012, 28, 17571-17577.

- 17. Hartono, D.; Xue, C. Y.; Yang, K. L.; Yung, L. Y. L. Decorating Liquid Crystal Surfaces with Proteins for Real-Time Detection of Specific Protein-Protein Binding. *Adv. Funct. Mater.* **2009**, *19*, 3574-3579.
- Lai, S. L.; Hartono, D.; Yang, K. L. Self-Assembly of Cholesterol DNA at Liquid Crystal/Aqueous Interface and Its Application for DNA Detection. *Appl. Phys. Lett.* 2009, 95, 153702.
- 19. McUmber, A. C.; Noonan, P. S.; Schwartz, D. K. Surfactant-DNA Interactions at the Liquid Crystal-Aqueous Interface. *Soft Matter* **2012**, *8*, 4335-4342.
- Sivakumar, S.; Wark, K. L.; Gupta, J. K.; Abbott, N. L.; Caruso, F. Liquid Crystal Emulsions as the Basis of Biological Sensors for the Optical Detection of Bacteria and Viruses. Adv. Funct. Mater. 2009, 19, 2260-2265.
- Lockwood, N. A.; Mohr, J. C.; Ji, L.; Murphy, C. J.; Palecek, S. R.; de Pablo, J. J.; Abbott,
 N. L. Thermotropic Liquid Crystals as Substrates for Imaging the Reorganization of
 Matrigel by Human Embryonic Stem Cells. Adv. Funct. Mater. 2006, 16, 618-624.
- Agarwal, A.; Huang, E.; Palecek, S.; Abbott, N. L. Optically Responsive and Mechanically Tunable Colloid-in-Liquid Crystal Gels That Support Growth of Fibroblasts. *Adv. Mater.* 2008, 20, 4804.
- Hsu, P.; Poulin, P.; Weitz, D. A. Rotational Diffusion of Monodisperse Liquid Crystal Droplets. J. Colloid Interface Sci. 1998, 200, 182-184.
- 24. Heppenstall-Butler, M.; Williamson, A. M.; Terentjev, E. M. Selection of Droplet Size and the Stability of Nematic Emulsions. *Liquid Crystals* **2005**, *32*, 77-84.

- Miller, D. S.; Abbott, N. L. Influence of Droplet Size, pH and Ionic Strength on Endotoxin-Triggered Ordering Transitions in Liquid Crystalline Droplets. *Soft Matter* 2013, 9, 374-382.
- 26. Hussain, A.; Semeano, A. T. S.; Palma, S. I. C. J.; Pina, A. S.; Almeida, J.; Medrado, B. F.; Pádua, A. C. C. S.; Carvalho, A. L.; Dionísio, M.; Li, R. W. C.; Gamboa, H.; Ulijn, R. V.; Gruber, J.; Roque, A. C. A. Tunable Gas Sensing Gels by Cooperative Assembly. *Adv. Funct. Mater.* 2017, 27, 1700803.
- 27. Khan, M.; Li, W.; Mao, S.; Shah, S. N. A.; Lin, J. M. Real-Time Imaging of Ammonia Release from Single Live Cells via Liquid Crystal Droplets Immobilized on the Cell Membrane. Adv. Sci. 2019, 6, 1900778.
- Verma, I.; Sidiq, S.; Pal, S. K. Protein Triggered Ordering Transitions in Poly (L-Lysine)-Coated Liquid Crystal Emulsion Droplets. *Liq. Cryst.* 2019, 46, 1318-1326.
- Dan, A.; Aery, S.; Zhang, S.; Baker, D. L.; Gleeson, H. F.; Sarkar, A. Protein Microgel-Stabilized Pickering Liquid Crystal Emulsions Undergo Analyte-Triggered Configurational Transition. *Langmuir* 2020, 36, 10091–10102.
- 30. Ortiz, B. J.; Boursier, M. E.; Barrett, K. L.; E., M. D.; Amador-Noguez, D.; Abbott, N. L.; Blackwell, H. E.; Lynn, D. M. Liquid Crystal Emulsions That Intercept and Report on Bacterial Quorum Sensing. *ACS Appl. Mater. Interfaces* **2020**, *12*, 29056-29065.
- 31. Guo, X. R.; Manna, U.; Abbott, N. L.; Lynn, D. M. Covalent Immobilization of Caged Liquid Crystal Microdroplets on Surfaces. *ACS Appl. Mater. Inter.* **2015,** *7*, 26892-26903.
- 32. Manna, U.; Zayas-Gonzalez, Y. M.; Carlton, R. J.; Caruso, F.; Abbott, N. L.; Lynn, D. M. Liquid Crystal Chemical Sensors That Cells Can Wear. *Angew. Chem. Intl. Ed.* **2013**, *52*, 14011-14015.

- 33. Carlton, R. J.; Zayas-Gonzalez, Y. M.; Manna, U.; Lynn, D. M.; Abbott, N. L. Surfactant-Induced Ordering and Wetting Transitions of Droplets of Thermotropic Liquid Crystals "Caged" inside Partially Filled Polymeric Capsules. *Langmuir* **2014**, *30*, 14944-14953.
- 34. Buck, M. E.; Lynn, D. M. Functionalization of Fibers Using Azlactone-Containing Polymers: Layer-by-Layer Fabrication of Reactive Thin Films on the Surfaces of Hair and Cellulose-Based Materials. *ACS Appl. Mater. Inter.* **2010,** *2*, 1421-1429.
- 35. Shimoni, O.; Yan, Y.; Wang, Y. J.; Caruso, F. Shape-Dependent Cellular Processing of Polyelectrolyte Capsules. *ACS Nano* **2013**, *7*, 522-530.
- 36. Fattorossi, A.; Nisini, R.; Pizzolo, J. G.; Damelio, R. New, Simple Flow-Cytometry Technique to Discriminate between Internalized and Membrane-Bound Particles in Phagocytosis. *Cytometry* **1989**, *10*, 320-325.
- 37. Gratton, S. E. A.; Ropp, P. A.; Pohlhaus, P. D.; Luft, J. C.; Madden, V. J.; Napier, M. E.; DeSimone, J. M. The Effect of Particle Design on Cellular Internalization Pathways. *Proc. Natl. Acad. Sci. U. S. A.* **2008**, *105*, 11613-11618.
- 38. Gupta, J. K.; Zimmerman, J. S.; de Pablo, J. J.; Caruso, F.; Abbott, N. L. Characterization of Adsorbate-Induced Ordering Transitions of Liquid Crystals within Monodisperse Droplets. *Langmuir* **2009**, *25*, 9016-9024.
- 39. Ray, A.; Nemethy, G. Micelle Formation by Nonionic Detergents in Water-Ethylene Glycol Mixtures. *J. Phys. Chem.* **1971,** *75*, 809-&.
- 40. Fernandez-Nieves, A.; Link, D. R.; Marquez, M.; Weitz, D. A. Topological Changes in Bipolar Nematic Droplets under Flow. *Phys. Rev. Lett.* **2007**, *98*, 087801.

For Table of Contents Use Only:

